→ DISCOVERY

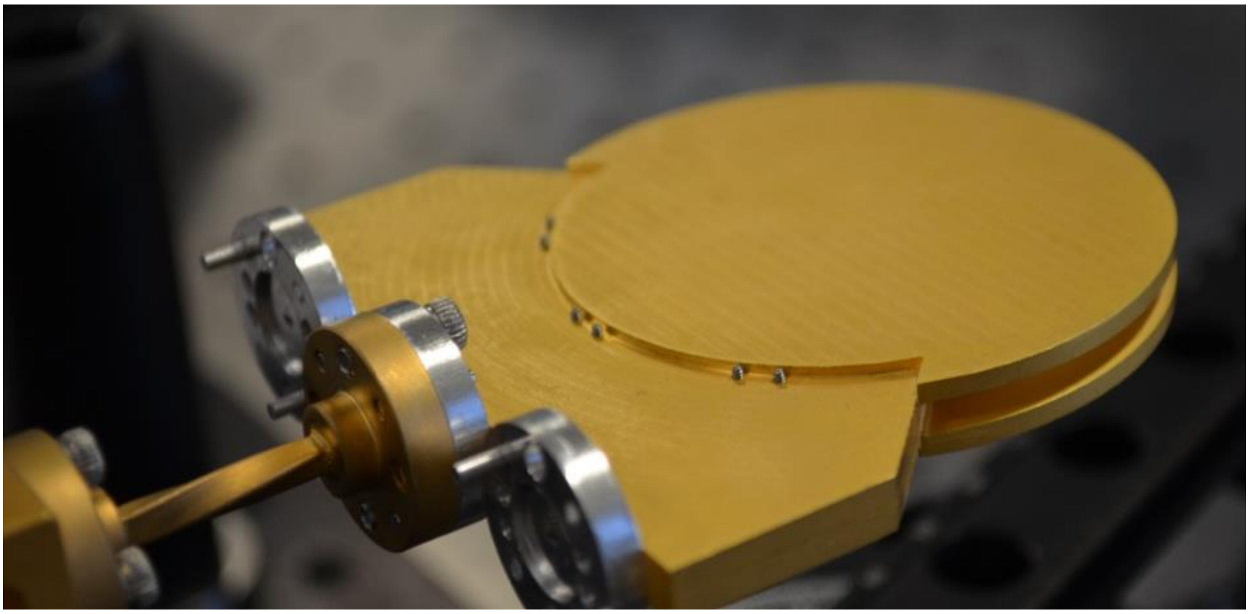

Sub terahertz geodesic lens antenna for imaging system

Executive summary

Early technology development

Open Discovery Ideas Channel

Affiliation(s): University of Bordeaux (Prime), KTH Royal Institute of Technology (Subcontractor)

Activity summary:

In this project, we propose a design of a geodesic antenna at 130 GHz and simulate it using FDTD methods. This antenna was then successfully fabricated and tested, exhibiting a 22 dB gain. Finally, this antenna was integrated on a non-destructive testing experiment, illustrating the advantage of multibeam in near field.

Publishing Date: 11/20/2023
Contract Number: <4000134617/21/NL/GLC/ov >
Implemented as ESA Standard Procurement

Table of content

PART 1 State of the art

1.1 Terahertz waves non destructive testing

1.1.1 Terahertz waves

THz waves, also called submillimeter waves, are electromagnetic waves in a frequency range between microwaves and infrared [1]. As shown in Figure 1, the THz range is between far infrared and millimeter waves, corresponding to frequencies between 0.1 THz and 10 THz, i.e. at wavelengths between 30 µm and 3 mm. The interest of THz waves lies in their specific interaction with matter. They can penetrate into non-metallic and non-polar materials, such as plastics, composite materials, plaster, wood, being harmless to the operator. These properties are promising for imaging the volume of opaque objects in order to detect defects, inclusions, infiltrations, delamination areas, humidity for example.

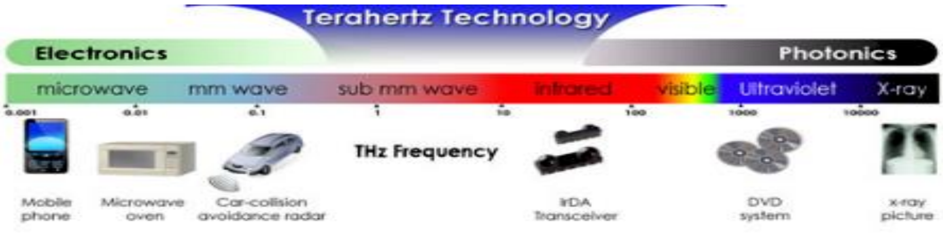

Figure 1 : Positioning of the terahertz domain in the electromagnetic spectrum

Several radar imaging applications have been demonstrated in the field of terahertz and submillimeter waves [2-4]. Due to the penetrating aspect of terahertz waves in polymer, plastic or composite materials, an application of non-destructive testing by radar imagery with frequency modulation in continuous mode (FMCW) can be envisaged on industrial objects allowing a complete 3D imaging of the structure of the scanned elements [5-7].

Gradient index lenses

1.1.1.1 General information on Luneburg lenses

A Luneburg lens is a lens with a symmetric index gradient. The refractive index n of a typical Luneburg lens decreases radially from the center to the outer surface. Each point on the surface of an ideal Luneburg lens is the focal point of the incident parallel radiation on the opposite side. Ideally, the dielectric constant of the material making up the lens goes from 2 at its center to 1 at its surface, with a variation depending on the radius. If the refractive index on the surface is the same as that of the surrounding medium, no reflection occurs on the surface. Inside the lens, the ray paths are arcs of ellipses.

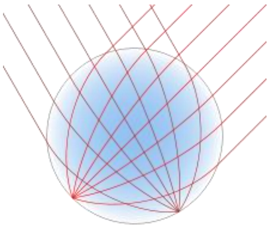

Figure 2 Luneberg lens concept

This property makes it possible to have a lens without aberrations and opens the way to certain applications in the microwave field. This can replace a parabolic reflector with a more compact system and manage several beams simultaneously. The lens can also be associated with a metal surface to make it a multi-directional reflector and make beacons for the maritime, aeronautical or space sectors.

1.1.1.2 Luneburg lenses at millimeter wave frequencies

The work carried out at the University of Bordeaux in 2011/2012 around Luneberg lenses aimed to assess how often solutions with index gradients could go up. From a geometric point of view, these lenses have radii between 3 and 10 cm, which is more than enough considering the wavelength to behave as in theory. FDTD simulations using CST software were performed, showing the possibility of using these devices.

Although optically functional, the losses which increase as the frequency increases have limited the interest of this solution. Use as a reflector can be easily achieved by a cube corner and the beam control functionality has not been achieved by other methods to date. Due to material losses at millimetric frequencies, this solution cannot therefore exceed ten GHz and there is no solution beyond 100 GHz.

1.1.2 Waterdrop lens antenna

Given the limits of Luneberg lenses due to the scattering induced by their material, the need to manage several beams in an integrated manner towards several transmitters / detectors is a problem which remains open for millimeter and terahertz frequencies. To address this issue, one solution is to use an antenna topology that has been demonstrated by the ESA in 2018 [13]. This geodesic lens is based on parallel flat waveguides which allows to have a compact device which generates several beams with an angular scan having a very wide interval. The proposed approach provides smooth lens profiles. Depending on the design, Gaussian beams or beams with special patterns can be generated, which can open the way to direct focusing after the lens. The shape of this wavy lens, resembling ripples of water drops, also called capillary waves on the surface of a fluid, hence the name waterdrop lens antenna.

This antenna therefore makes it possible to generate several beams. It can be seen that the antenna operates from -75 to + 75 °. Beyond the losses of gain are visible. This range of 150 ° remains a very large value, including in comparison to conventional Luneburg lenses which are generally used in this range of angles.

1.1.3 Millimeter wave antenna for terahertz NDT

Similarly, to telecommunications requirements at millimeter frequencies, it may be advantageous to be able to control a beam so as to probe space, a medium, an object or a target with a beam scan. For this, we can identify an interest to manufacture drop antennas at 60 GHz, 122 GHz and 300 GHz, which correspond to frequencies of interest for imaging, non-destructive testing and 5G telecom (and 6G for sub- millimeters).
Based on the existing transceivers and giving the NDT transmission, resolution and overall performance, the best frequency is the D-band.

The heart of the project is to offer a multi-beam solution which is not limited in frequency by the diffusion effects in plastic materials such as index gradient lenses.

PART 2 Technology design and test

2.1 Simulations

2.1.1 Antenna structure

The geodesic antenna with a diameter of five cm is made following the waterdrop antenna design, by the assembly of two microfabricated pieces, the bottom layer and the top layer, as illustrated on Figure 3. The FDTD simulation, performed using CST Microwave Studio, are done for each port. Three WR6 ($(1.651 * 0.8255\ mm)$ ports (port 0, 1 and 2) corresponds to three radiation patterns (40°, 0° and -40°). They are separated by a distance of 22.3 mm, larger than the width of the UG-387/U flange 19.05 mm. Frequency of operation is from 128 to 132 GHz ($\lambda \approx 2.3\ mm$).

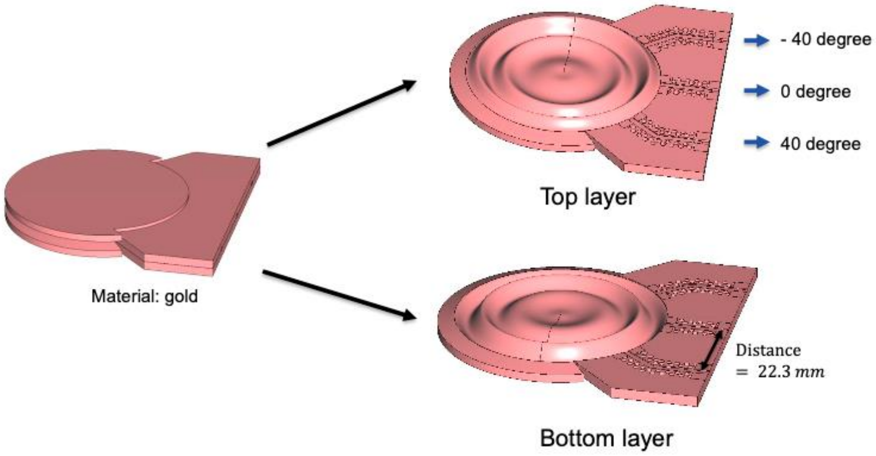

Figure 3 : Antenna structure with two pieces

While the diameter of the geodesic lens is 50mm, it comes to 58 mm including a geodesic horn. The port area width is 70 mm. The proposed design includes three rectangular waveguides from the flange to the antenna. In order to prevent any leakage, EBG holes are added along the waveguide (Figure 4). This solution implies the presence of an air gap of 30µm between the bottom and top layers. Then, four screws per waveguide (12 in total) are used for the lens assembly.

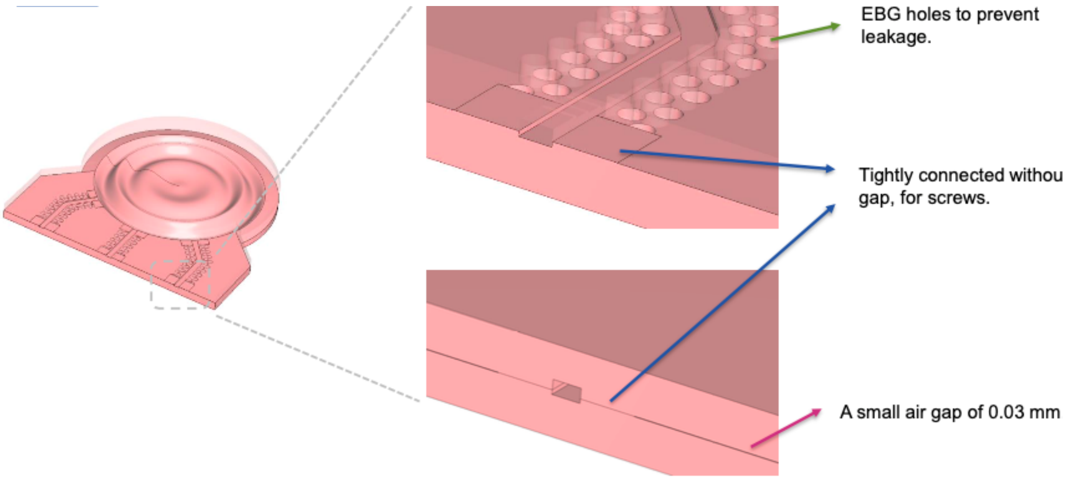

Figure 4 : Waveguide from port to antenna structure

2.1.2 Simulated Angular performance

The angular performance of the geodesic antenna is simulated using the CST Microwave Studio radiation pattern results. It corresponds to signal at infinity as a function of the angle. We obtain peaks at -40°, 0° and 40° for ports 0, 1 and 2, with similar pattern from 128 to 132 GHz.

2.1.3 Angular performance simulation like the experimental setup

Since the experimental setup is limited in distance, and since the detector has a non-negligible surface, we extract from the simulation the electrical field (absolute) and we calculate the expected pattern based on the real experiment. In the experiment, (detailed bellow), the detector distance is 12.5cm and the detector size is 2cm. The simulated radiation shape presented for comparison in the experimental section will be based on that approach.

2.2 Measurements

Measurements are S parameters and radiation pattern. We can see on Figure 7 that the reflection coefficient is below -15 dB in the frequency band of interested. Then, we can see on Figure 8 that the radiation patterns exhibits a gain of more than that 22dB, which is beyond the state of the art at that frequency. This **is an important and key result of this study and validate the concept of this project.**

These measurements are in good agreement.

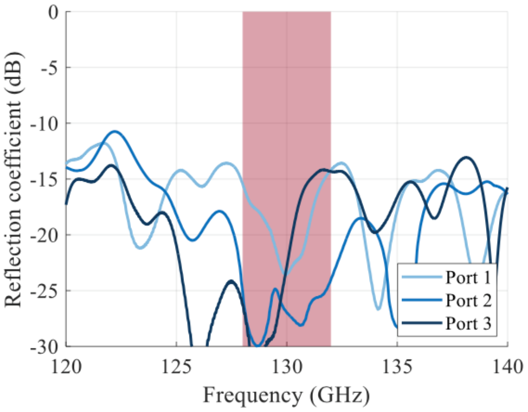

Figure 5 : S parameters

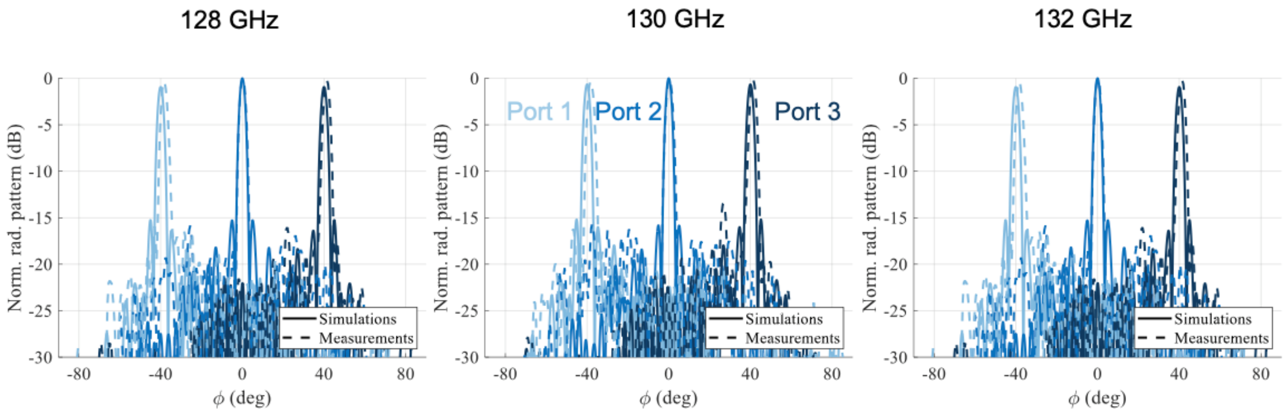

Figure 6 : Radiation patterns

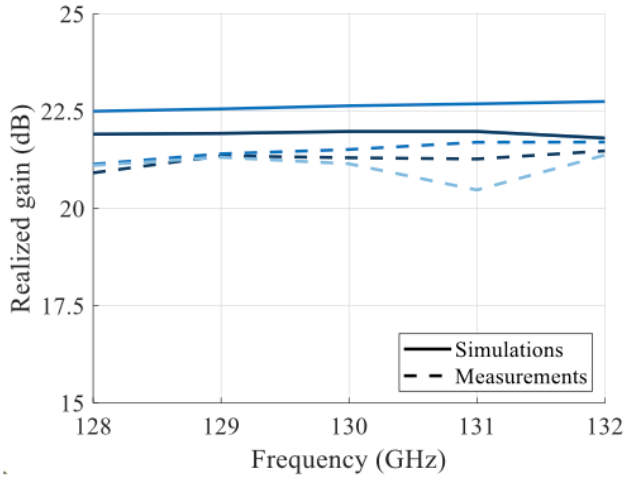

Figure 7 : Gain of the three ports with clamp optimization

Based on this last optimal configuration, 3D pattern were measured (Figure 8 and Figure 9) and we obtain as expected azimuthal directivity for each port.

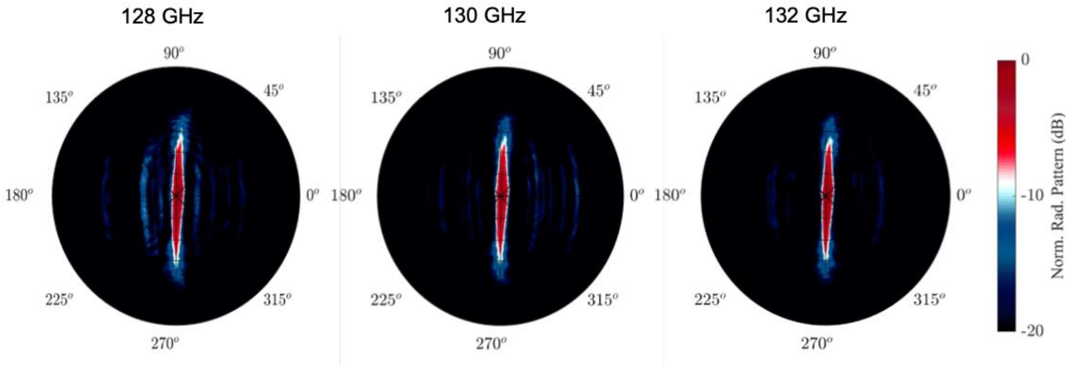

Figure 8 : 3D pattern with a goniometric measurement of the port 2

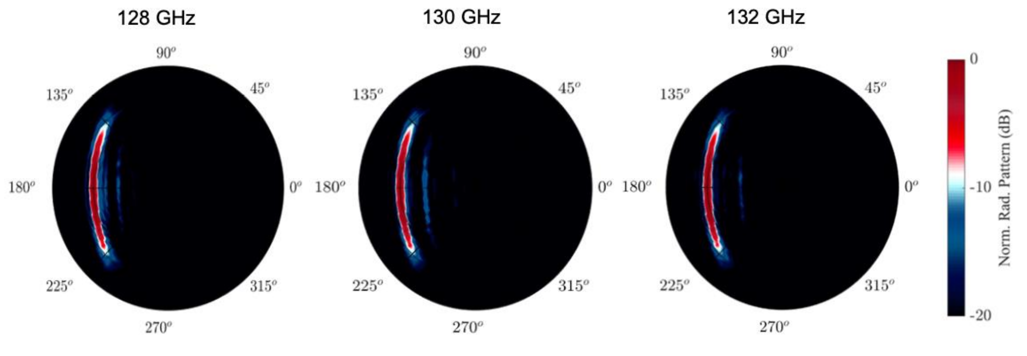

Figure 9 : 3D pattern with a goniometric measurement of the port 1

Several iteration and measurement finally allowed to get high directivity for each beam, more than 21dB gain and reflection coefficient below -15 dB.

PART 3 Antenna integration for nondestructive testing

3.1 Experimental setup (summer 2023)

The proposed application is the analysis of a hydrogen tank. We propose an original approach which highlights the specificity of the antenna, by making this measurement from the inside. That do not correspond here to real application case, but it could be used for any curved object and the goal is to demonstrate a radial multi beam imaging application with a representative object. This approach is not usual, because the usual systems are either systems doing plane scans, or robotic systems that can follow a curved surface, but there is no system that can manage several beams from an antenna in the terahertz domain. To facilitate this demonstration measurement in the laboratory, we put aluminium foil markers on the outside of the tank, so as to see them and reconstruct the image.

The setup consists of an 80 cm motor coupled to the geodesic antenna making a linear measurement, being placed in the centre of the device. Since we only have one radar working at that frequency, this measurement is repeated three times by connecting the radar to the three ports and moving the radar with a translation between each measurement, to maintain the position of the antenna with respect to the sample.

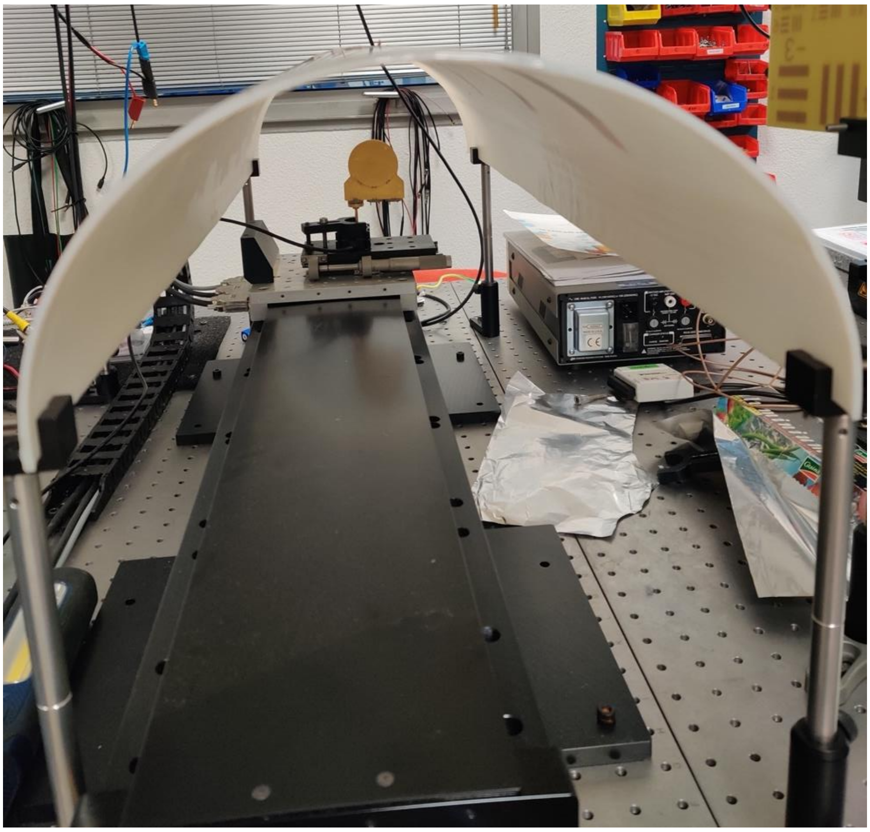

Figure 10 ; Experimental setup : The antenna is translated along the 600 mm tank

Since the FMCW radar allow to get several reflected echoes, we get the data corresponding to the distance between the antenna and the object, and we plot that as a function of the position along the object under investigation. We can observe peaks corresponding to foil markers on the outside of the object.

This measurement is performed for each antenna, and plotted as a heatmap in Figure 11. We can see that all the markers are detected

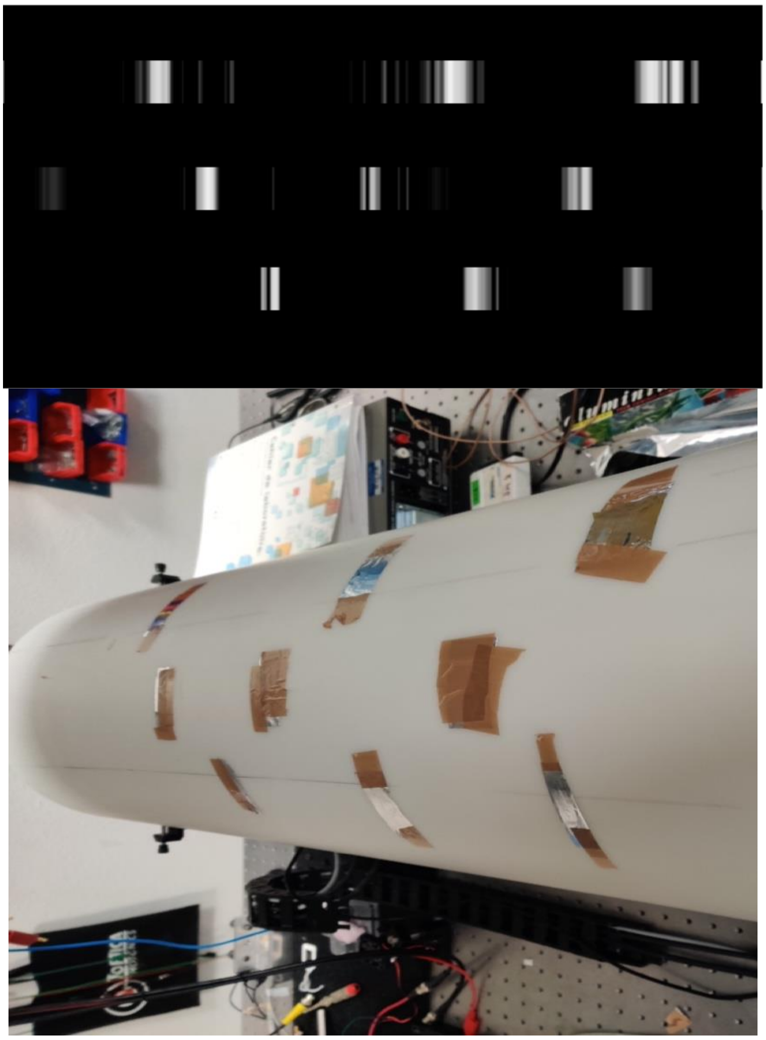

Figure 11 : (top) 2D flattened heat map of the reflected signal (bottom) Photography of the object and its markers. We can see the same position of the measured peaks and markers.

This measurement demonstrates the near field imaging application and the possibility to use such antenna for non-destructive testing, as illustrated on 3D reconstruction in Figure 16.

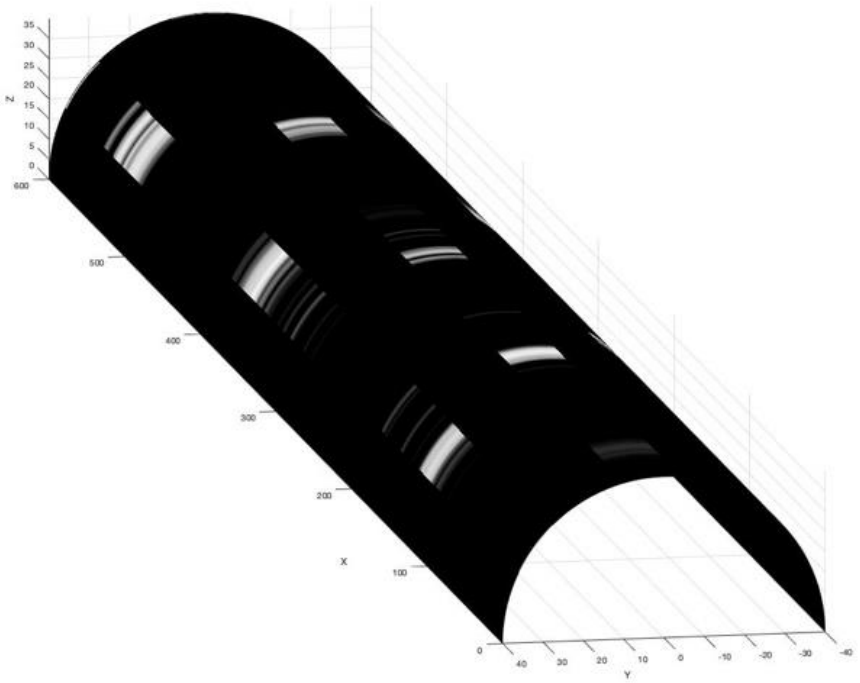

Figure 12 : 3D view of the reconstructed signal from the geodesic antenna in the non destructive testing configuration

Conclusion

Thanks to this project, we successfully demonstrate the design, fabrication, test and integration of a multiport geodesic lens at 130 GHz with a measured gain of 22 dB.

This first demonstration is carried out with three ports, which makes it possible to confirm the operating principle of the antenna at TRL 4. This project also showed that although being physically comparable to an antenna operating at 30 GHz, the manufacture of a 130 GHz antenna requires a high level of precision, adjustments having made it possible at the end of the project to improve the antenna's performance by several dB.

We obtain **performances that go beyond the state of the art**, and to have experimental results in agreement with the simulations.

Finally, the integration of the antenna in a near field experiment taking advantage of the topology of the antenna opens interesting perspectives for a possible future antenna with more ports. This experiment showed that it was possible to **scan curved objects by only making a translation** movement without following the curvature, the different beams making it possible to scan each angle.

Since TRL3-4 is now demonstrated, further development could be done at that frequency range with this antenna size, and here are some ideas:

- While the choice to limit to three WR6 ports was made for conservative motivation, we should now increase the number of ports and use cost effective transceivers to take full profit of this topology.
- Nondestructive measurement at different distances, including large objects (more than one meter) could be carried out.
- Dual application including mmW data link could be explored in combination with FMCW mmW radar.
- Advanced processing as synthetic aperture radar could the adjusted to this design, in order to increase the resolution.

Then other developed could be also done:

- Since there is not scattering limitation like dielectric Luneberg lenses, higher frequency lens could be fabricated, reaching the terahertz range (typically 300 GHz and then 600 GHz).
- Large antenna for higher gain could also be explored, to evaluate the physical limits for high gain schemes.

PART 4 Bibliography

[1] Guillet, J. P., Recur, B., Frederique, L., Bousquet, B., Canioni, L., Manek-Hönninger, I., ... & Mounaix, P. (2014). Review of terahertz tomography techniques. Journal of Infrared, Millimeter, and Terahertz Waves, 35(4), 382-411.

[2] A. O. Chulkov, L. Gaverina, C. Pradere, J.-C. Batsale, and V. P. Vavilov, “Water detection in honeycomb composite structures using terahertz thermography,” Russ. J. Nondestruct. Test., vol. 51, pp. 520–523, 2015.

[3] Ospald, F., Zouaghi, W., Beigang, R., Matheis, C., Jonuscheit, J., Recur, B., ... & González, L. V. (2013). Aeronautics composite material inspection with a terahertz time-domain spectroscopy system. Optical Engineering, 53(3), 031208.

[4] M. Vandewal et al., “Structural Health Monitoring using a Scanning THz System,” IEEE, pp. 1–2, 2013.

[5] Guillet, J. P., Wang, K., Roux, M., Fauquet, F., Darracq, F., & Mounaix, P. (2016, September). Frequency modulated continuous wave terahertz imaging for art restoration. In Infrared, Millimeter, and Terahertz waves (IRMMW-THz), 2016 41st International Conference on (pp. 1-1). IEEE.

[6] C. L. K. Dandolo, J.-P. Guillet, X. Ma, F. Fauquet, M. Roux, and P. Mounaix, “Terahertz frequency modulated continuous wave imaging advanced data processing for art painting analysis,” Opt. Express, vol. 26, no. 5, p. 5358, Mar. 2018.

[7] F. Friederich et al., “Terahertz Radome Inspection,” Photonics, vol. 5, p. 1, 205

[8] FP7 Projet Dotnac report : https://cordis.europa.eu/project/rcn/96573/reporting/en

[9] Smolyanskaya, O. A., Chernomyrdin, N. V., Konovko, A. A., Zaytsev, K. I., Ozheredov, I. A., Cherkasova, O. P., ... & Coutaz, J. L. (2018). Terahertz biophotonics as a tool for studies of dielectric and spectral properties of biological tissues and liquids. Progress in Quantum Electronics.

[10] Coutaz, J. L. (2012). Optoélectronique térahertz. EDP Sciences.

[11] Sleiman, J. B., El Haddad, J., Perraud, J. B., Bassel, L., Bousquet, B., Palka, N., & Mounaix, P. (2014, September). Qualitative and quantitative analysis of explosives by terahertz time-domain spectroscopy: application to imaging. In Infrared, Millimeter, and Terahertz waves (IRMMW-THz), 2014 39th International Conference on (pp. 1-2). IEEE.

[12] Terahertz Components & Systems: Technology and Market Trends , https://tematys.fr